CHARACTERISTICS OF TURBULENT NONPREMIXED JET-FLAMES AND JET-FLAMES IN CROSSFLOW IN NORMAL- AND LOW-GRAVITY

N. T. Clemens, I.G. Boxx, C.A. Idicheria
Department of Aerospace Engineering and Engineering Mechanics, The University of Texas at Austin, Austin, TX 78712-1085

INTRODUCTION

It is well known that buoyancy has a major influence on the flow structure of turbulent nonpremixed jet flames. For example, previous studies have shown that transitional and turbulent jet flames exhibit flame lengths that are as much as a factor of two longer in microgravity than in normal gravity.[1-2] The objective of this study is to extend these previous studies by investigating both mean and fluctuating characteristics of turbulent nonpremixed jet flames under three different gravity levels (1 g, 20 mg and 100 μg). This work is described in more detail elsewhere.[3-5]

In addition, we have recently initiated a new study into the effects of buoyancy on turbulent nonpremixed jet flames in cross-flow (JFICF). Buoyancy has been observed to play a key role in determining the centerline trajectories of such flames.[6] The objective of this study is to use the low-gravity environment to study the effects of buoyancy on the turbulent characteristics of JFICF. This work is described in more detail in Ref. 7.

EXPERIMENTAL APPARATUS/CONDITIONS

The low-gravity experiments were conducted in the University of Texas 1.25 second drop tower and the NASA GRC 2.2 second drop tower. Figure 1 shows a solid model of the drop-rig used in both towers. The drop-rig uses an aluminum frame (38"×16"×36") that is covered on each side with 0.08" aluminum sheet-metal. In the jet-flame experiments the jet issued into the quiescent air in the interior of the drop rig. The fuel jet was delivered from a 1.75 mm (inner diameter) stainless steel tube, with a 25.4 mm diameter concentric, premixed, methane-air flat-flame pilot. Fuel for the jet was stored in two onboard, 18.3 in^3 stainless steel pressure vessels. The flow rate was controlled with line pressure regulators upstream of choked micro-metering valves.

The JFICF experiments used the same basic drop rig, but the rig was equipped with a blow-through cross-flow section (8"×8"×24") as shown in Fig. 1. A round jet of ethylene issues from a 1/8" diameter circular orifice mounted flush with one wall of the test section. The cross-flow is driven by two DC-powered axial, in-line blowers. The cross-flow velocity can be set to 0.94 m/s or 1.32 m/s by using one or two blowers, respectively.

For both flow configurations, the flame luminosity was imaged using a Pulnix TM-6710 progressive scan CCD camera, capable of operating at 235 fps or 350 fps at resolutions of 512×230 pixels and 512×146 pixels, respectively. The camera was electronically shuttered, with the exposure time depending on flame luminosity (1/235 to 1/2000 seconds), and the field of view was typically 405mm in the streamwise direction. The drop-rig was controlled by an onboard computer (CyberResearch Inc). Three different jet fuels were studied in the jet flame experiments: propane, ethylene and methane. These experiments were conducted over Reynolds numbers (based on jet-exit conditions) ranging from 2000 to 10500. The Becker & Yamazaki[8] "buoyancy parameter" $\xi_L=Ri_s^{1/3}L_f/D_s$ (where $Ri_s=gD_s/U_s^2$ is the source Richardson number based on the source diameter $D_s=D(\rho_o/\rho_\infty)^{1/2}$, and source velocity $U_s=U_o$, L_f is the average visible flame length, ρ_o is the jet fluid density and ρ_∞ is the ambient density) for these flames ranged from 0.22 in microgravity up to 12 in

normal gravity. In all JFICF cases the fuel was ethylene. The momentum flux ratio ($r = \sqrt{(\rho_j u_j^2/\rho_{cf} u_{cf}^2}$), where the subscripts refer to the jet and cross-flow conditions, respectively) ranged from 6 to 10, and Reynolds numbers ranged between 3000 and 5000. Two cases were chosen so as to compare two JFICF of identical momentum flux ratio but different jet exit Reynolds numbers. Two other cases were chosen so as to maintain a constant jet-exit Reynolds number at two different momentum flux ratios.

RESULTS AND DISCUSSION

Jet Flames -- The RMS fluctuations of flame luminosity were computed from the instantaneous luminosity images. Figure 2 shows RMS images for ethylene and propane flames at a range of Reynolds numbers and where the buoyancy has been quantified with ξ_L. This figure shows that flames with similar ξ_L have similar fluctuations, which indicates that ξ_L does an excellent job of quantifying the level of buoyancy. Large fluctuations are present near the flame tip in the large ξ_L (buoyant) flames, whereas small ξ_L flames exhibit the largest fluctuations off centerline near the regions of high shear. These results further suggest that the structure of the large-scale turbulence reaches its momentum-driven asymptotic state for values of ξ_L less than about 2-3.

Figure 3a shows the variation of the normalized mean visible flame length for each of the jet flame cases studied. It is evident from the figure that the flame lengths are essentially the same under the different gravity levels at the highest Reynolds numbers. For comparison, Fig. 3a also shows the data of Hegde *et al.*[1,2] for propane flames under normal and microgravity. It is clear that we do not observe the large differences in flame lengths with g-level that were observed in their studies. To provide some validation of our 1g data, Fig. 3b shows the current 1g data plotted with those of Becker and Yamazaki[8] and Mungal *et al.*[9] It can be seen that our data are in excellent agreement with these previous 1g studies.

Volume rendering of jet flame image sequences was used to investigate the large-scale structure characteristics. In this technique, 3-D isocontours (x,y,t) of the jet flame edge are generated from the luminosity images, allowing comparisons of such features as large-scale structure evolution and propagation velocity (celerity). Figure 4 shows a plot of the ratio of celerity to jet exit velocity, U_s/U_o (%), against the buoyancy parameter, ξ_L. The normal gravity flames (i.e. those with high ξ_L values) are associated with higher celerity. This suggests that celerity is in fact buoyancy dependent, contrary to the findings of Mungal *et al.*[9], who found the celerity to be 12 ± 2% of the jet exit velocity irrespective of ξ_L and fuel type. For $\xi_L < 4$, the celerity appears to become independent of the gravity level and fuel type. In this regime, there is reasonable agreement with the findings of Mungal *et al.*[9]

Jet Flames in Crossflow -- Figure 5 shows typical time-sequence luminosity images of the JFICF under normal- and low-gravity conditions. In the JFICF image sequences, we observe that the jet shear-layer vortices tend to be wider and slower to roll up in low-gravity than in normal-gravity. Jet flames exhibit a similar broadening in low-gravity. The deeper penetration of unburned air into the JFICF in normal-gravity than in low-gravity seen in these images was characteristic of all JFICF cases run. Volume rendering and frame-by-frame analysis revealed a greater degree of spatial and temporal uniformity and coherence in the shear-layer vortex behavior in low-gravity compared to those in normal-gravity.

Figure 6 shows the centerline trajectories for the JFICFs, plotted in log-log scale. We specify the centerline as the midpoint of each line in a threshholded, ensemble average of 600 instantaneous luminosity images. Using linear regression analysis, we fit each trajectory to a power-law formula of the form $z/rd = A(x/rd)^n$, where z is the coordinate in the direction of the jet and x is the coordinate

in the direction of the cross-flow. The trajectories are based on data limited to x/rd > 2 due to the low luminosity of the near-field region. In all eight cases, the exponent of the power-law ranged from 0.18 to 0.21. This is in reasonable agreement with the correlation of Huang and Chang[10] for the far-field trajectory of a propane JFICF. In no case did the non-buoyant JFICF follow the 0.33 power scaling characteristic of non-reacting jets in cross-flow. This plot also illustrates a systematic departure from power-law scaling in the far-field in every normal-gravity JFICF case, a trend not seen in any of the low-gravity JFICF cases. We conclude this departure from power-law scaling is due to buoyancy-induced acceleration of the hot combustion products in the far-field region.

ACKNOWLEDGEMENTS

This research is supported under co-operative agreement NCC3-667 from the NASA Microgravity Sciences Division with Dr. Zeng-Guang Yuan of NCMR as technical monitor.

REFERENCES

1. Hegde, U., Zhou, L., Bahadori, M. Y., *Combust. Sci. Technol.* 102:95-100 (1994).
2. Hegde, U., Yuan, Z.G., Stocker, D.P. and Bahadori, M.Y., *Proc. of Fifth International Microgravity Combustion Workshop*, pp. 259-262 (1999).
3. Idicheria, C.A., Boxx, I. G., Clemens, N.T. AIAA Paper 2001-0628 (2001).
4. Clemens, N.T., Idicheria, C.A. and Boxx, I.G., Proc. of Sixth International Microgravity Combustion Workshop, pp. 133-136 (2001).
5. Idicheria, C. A., Boxx, I. G., Clemens, N. T., Proceedings of the Third Joint Meeting of the U.S. Sections of the Combustion Institute (2003).
6. Kuppu Rao, V. and Brzustowski, T. A., *Combust. Sci. Technol.* 27: 229-239 (1982).
7. Boxx, I. G., Idicheria, C. A., Clemens, N.T. AIAA Paper 2003-1151 (2003)
8. Becker, H. A. and Yamazaki, S., *Combust. Flame* 33: 123-149 (1978).
9. Mungal, M.G., Karasso, P.S. and Lozano, A., *Combust. Sci. Technol.* 76:165-185 (1991).
10. Huang, R. F. and Chang, J. M., *Combust. Flame* 98: 267-278 (1994).

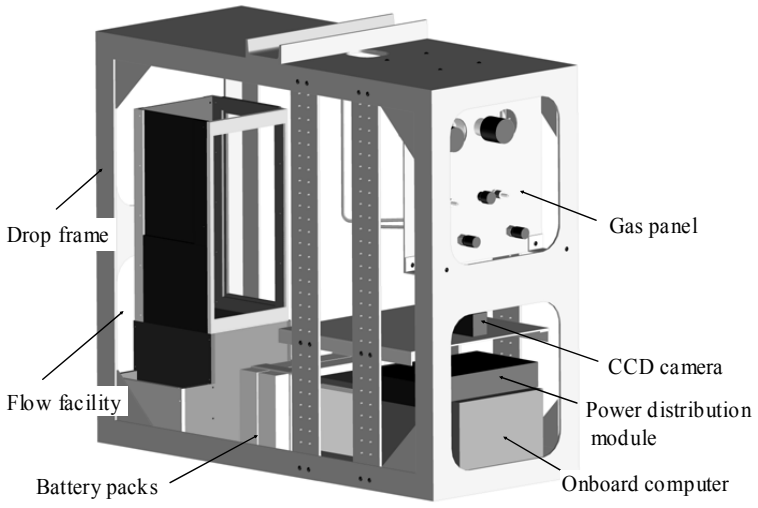

Figure 1. Schematic of the turbulent nonpremixed jet-flame drop rig.

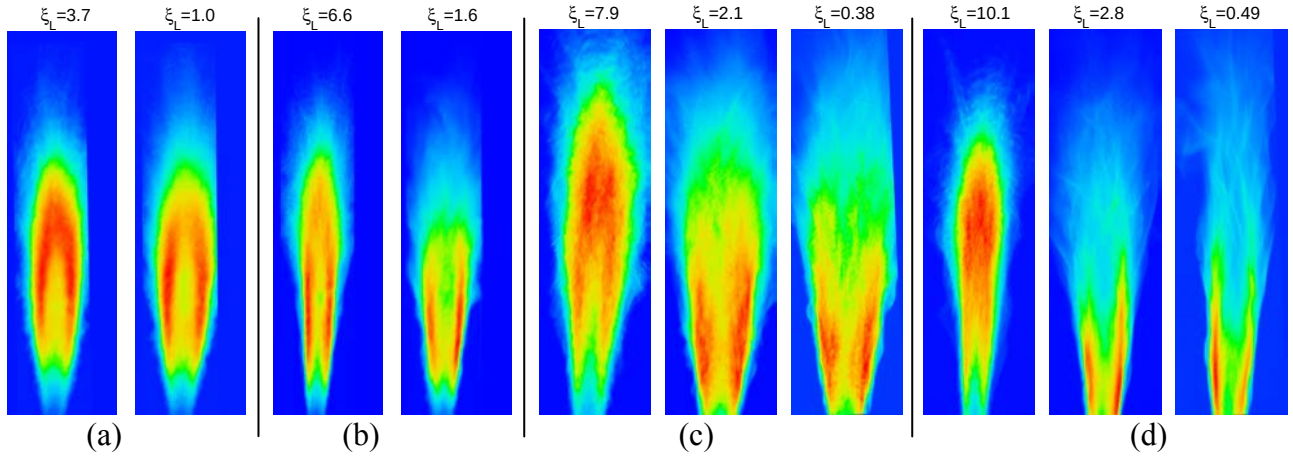

Figure 2. Sample RMS luminosity images: (a) Ethylene Re_D=10,500, 43<x/D<279, (b) Ethylene Re_D=5000, 43<x/D<279, (c) Propane Re_D=8500, 76<x/D<308, and (d) Propane Re_D=5000, 76<x/D<308.

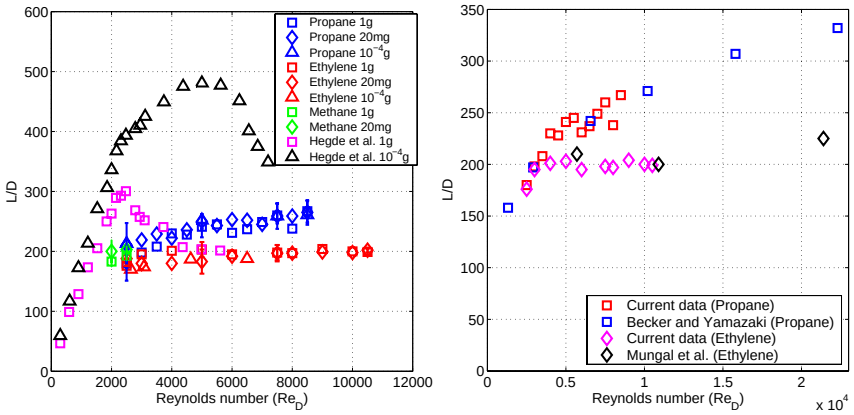

Figure 3. Flame length data. (a) 1g and low-g. (b) 1g only.

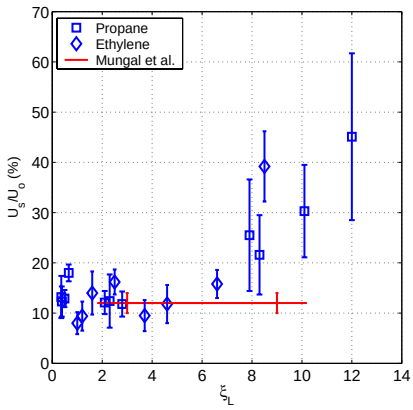

Figure 4. Jet flame structure celerity.

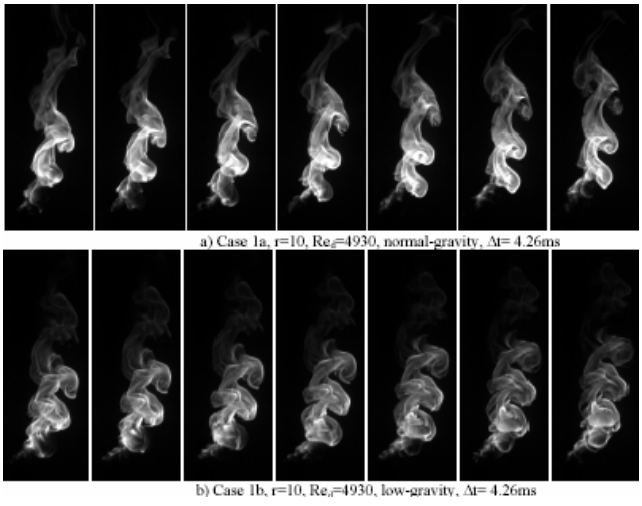

Figure 5. JFICF – Instantaneous time-sequenced images for JFICF with Re_d=4930, r=10. (a) 1g, (b) low-g.

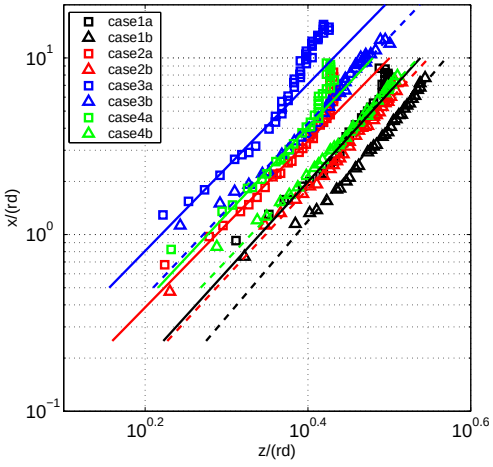

Figure 6. JFICF centerline trajectories. (Square symbols 1g, triangles low-g)